Smart Plaster of Paris Developed for Real-Time Monitoring of Orthopedic Casting and Multiple Infrastructure Applications Using Vipulanandan Models

A. R. Maddi and C. Vipulanandan,
Center for Innovative Grouting Materials and Technology (CIGMAT)
University of Houston, Houston, Texas 77204-4003.
Chandra Mohan, Biomedical Engineering, University of Houston, Houston, Texas

Abstract

Based on the physical and thermal properties, Plaster of Paris (P-O-P) has been used in many applications including the medical field and infrastructure constructions for over thousands of years around the world. **With the increased applications developing new technology to real-time monitor the changes from slurry to the solidified materials are important for evaluating the curing processes and the performances under various applications.** Based on the **newly developed Vipulanandan** electrical characterization **method,** the resistivity was identified as the critical material property for the P-O-P with water-to-binder ratio of 0.5. In order to make the highly sensing piezoresisitive P-O-P, **another innovative approach**, up to 0.05% of carbon fibers (CF) were added and tested. The measured initial resistivity immediately after mixing was sensitive to the amount of carbon fiber addition. During curing the changes in resistivity were monitored using the two probe method and alternative current at 300 kHz. During curing the resistivity changes were sensitive to the amount of fibers added to the P-O-P and was modeled using the Vipulanandan Curing Model. Solidified P-O-P with and without carbon fibers were tested under compressive loading after 1, 7 and 28 days of curing under the room condition (23^{o}C and relative humidity of 50%). The one day and 28 days the average compressive strengths of P-O-P without fibers were 2.14 MPa and 6.04 MPa respectively. The piezoresistive compressive strain at failure for the P-O-P without CF were less than 1% and with the addition of 0.02% and 0.05% CF it not only increased the compressive strength but also substantially increased the piezoresisitive compressive axial strain at peak stress. **After 28 days of curing, the P-O-P with 0.05% CF the axial piezoresistive strain at the peak stress was 345%, it increased by over 500 times (50,000%) compared to the P-O-P without CF, clearly showing the very high sensitivity of the P-O-P develop in this study with CF addition (smart P-O-P).** Vipulanandan Piezoresistive p-q Model was used to predict the piezoresistive behavior of the **smart** P-O-P and it predicted the behavior very well based on the root mean square error (RMSE). Vipulanandan Correlation Model was used to predict the changes in the compressive strength and compressive piezoresisitive failure strain with curing time **and also the long-term property limits were predicted**.

1. Introduction

In the medical and veterinary fields, cementitious, polymers and composite materials are commonly used as orthopedic cast material [Parmar et al. 2014, Stefanie, et al. 2011, Lewry et al. 1994]. Plaster of Paris (POP) is the traditional cementitious material used for casting. It is considered the most versatile of splinting materials, is completely moldable and can withstand considerable forces [Stefanie, et al. 2011]. One notable downside of this cast is that the hardening process is an exothermic process. In some cases, these exothermic processes can cause temperatures to rise to dangerous levels and cause thermal injury. Other disadvantages include high water permeability and setting times. An important clinical need is to be able to assess the status of the injured tissue beneath the cast in real time, which itself could cause changes in temperature or moisture. Gypsum or partially dehydrated

gypsum (Plaster of Paris (POP)) is considered as one of the oldest construction material that has been used for thousands of years around the world. Also Egyptians as well as Romans have used it for plastering walls however not more is known on plaster used after the end of Roman occupation.

Plaster of Paris takes its name from Paris, France, where it was first widely used chemically, surgically and in construction works (Browner et al., 2008). Plaster of Paris is produced by removing the impurities from the mined gypsum and then heating it under controlled conditions to reduce the amount of water of crystallization (Szostakowski, et al., 2017).
The increasing concerns related to environmental impacts of manufacturing of Portland cement at very high temperature (1400^{o}C) and the emission of carbon dioxide during the process, resulting in higher cost of manufacturing and also transportation. Hence there is increasing interest in using alternative materials for construction and maintenance.

The availability of POP as a natural gypsum material and also a byproduct from several chemical industries has made it gain momentum during the past few decades around the world.

Plaster of Paris ($2CaSO_4.H_2O$) is calcium sulphate with water. It is prepared by heating gypsum ($CaSO_4.2H_2O$) at 120°C to allow partial dehydration. When mixed with water, it gives out heat and quickly sets to a hard-porous mass within 5 to 15 minutes. The first step is called the setting stage with a slight expansion in volume. The second stage is the hardening stage.

Stage 1: Heating gypsum at 120 ℃

$$2(CaSO_4 \cdot 2H_2O) \xrightarrow{\Delta} 2\,(CaSO_4 \cdot \tfrac{1}{2}\,H_2O) + 3\,H_2O \qquad (1)$$

Stage 2: Plaster of Paris mixed with water

$$2(CaSO_4 \cdot \tfrac{1}{2}\,H_2O) + 3\,H_2O \rightarrow 2\,(CaSO_4.2H_2O) + \text{Heat} \qquad (2)$$

So theortrically minimum of 18.6 grams of water is added to 100 grams of POP powder, water to-binder ration of 0.186, to hydrate it into a solid. Based on the applications varying amounts of water-to-POP is used to mix well with the water, control the rheological properties and hardening process.
Because of its light weight, low density, its acceptable Mechanical properties, these new materials are recommended for exploitation in the manufacturing of popular lightweight construction finishing like panels for ceiling or walls and other applications.

2. Objectives

The focus **of this study** was to develop and characterize highly sensing plaster of Paris (P-O-P) material and also **develop** a nondestructive electrical method for real-time monitoring. Following are the **specific** objectives:
(i). Identify the electrical property for the P-O-P material which can be used for real-time monitoring.
(ii). Monitor and model the curing of the P-O-P with and without varying CF contents.
(iii). Develop and characterize the piezoresistive response of the **P-O-P with and without varying CF contents.**

(iv). Model the piezoresistive behavior and the changes in the multiple properties with curing time using the Vipulanandan Models.

3. Materials and Methods

Material Preparation

Commercially available Plaster of Paris (POP) was used. The water-to-plaster binder ratio used was 0.5. The Plaster of Paris slurries were prepared by hand mixing and adding the POP in three stages into the water. After mixing, POP specimens were prepared using cylindrical molds 50 mm in diameter and 100 mm in height. Also four wires were placed in the mold to monitor the electrical resistance changes.

Methods of Testing

Compression Test

The cylindrical specimens (50 mm diameter and 100 mm height) were capped and tested at a predetermined controlled displacement rate of 0.01 mm/min. Compression tests were performed on POP samples after 1 day, 7 days and 28 days of curing using a hydraulic compression machine.

Modeling

Vipulanandan Curing Model

To characterize the curing with the resistivity changes in the hardening P-O-P, Vipulanandan Curing Model was used and the relationship is defined as follows **[17, 18, 21]**:

$$\frac{1}{\rho(t)} = \left(\frac{1}{\rho_{min}}\right)\left[\frac{\left(\frac{t+t_o}{t_{min}+t_o}\right)}{q_1+(1-p_1-q_1)*\left(\frac{t+t_o}{t_{min}+t_o}\right)+p_1*\left(\frac{t+t_o}{t_{min}+t_o}\right)^{\frac{q_1+p_1}{p_1}}}\right] \quad (5)$$

where $\rho\ (t)$ is electrical resistivity that changes with the curing time (t), minimum electrical resistivity is ρ_{min}, t_{min} is time to reach the minimum electrical resistivity. The model parameters are p_1 and q_1 and t_0. The ρ_{min} and t_{min} are time independent model parameters that will explain the changes occurred due to the addition of the CF materials to the P-O-P and the curing conditions.

Vipulanandan Piezoresistive p-q Model

The Piezoresistivity behavior of the POP with and without carbon fibers was modeled using the Vipulanandan Piezoresistive p-q model (Vipulanandan 2021) and is defined as follows:

$$\sigma = \frac{\sigma_{max} \times \left(\frac{\left(\frac{\Delta\rho}{\rho}\right)}{\left(\frac{\Delta\rho}{\rho}\right)_0}\right)}{q_2 + (1-p_2-q_2) \times \left(\frac{\left(\frac{\Delta\rho}{\rho}\right)}{\left(\frac{\Delta\rho}{\rho}\right)_0}\right) + p_2 \times \left(\frac{\left(\frac{\Delta\rho}{\rho}\right)}{\left(\frac{\Delta\rho}{\rho}\right)_0}\right)^{\left(\frac{p_2+q_2}{p_2}\right)}}, \quad (3)$$

where σ_{max} is the maximum stress at failure, $(\Delta\rho/\rho)_0$ is the piezoresistivity of the hardened cast material under the maximum stress, (Δρ/ρ) is the piezoresistive strain at any stress σ and p_2 and q_2 are the model parameters influence by the composition of the material, material properties and testing environment.

4. Results and Discussions

Density

The specific gravity of the POP powder was 2.54 (manufacture's data sheet). The density of the POP samples prepared with water-to-binder ration of 0.5 with and without carbon fibers was 1.68 g/cc at the time of mixing and the initial porosity was 0.56. The specimens were cured under room condition The density was 1.41 g/cc after 7 days of curing and 1.24 g/cc after 28 days of curing, indicating the loss in moisture during curing [9].

SEM Analyses

It was important to characterize the physical properties and chemical composition of the POP powder used in this study.

Physical and Chemical Properties

Physical Properties

The shapes and sizes of POP particles are shown in Figure 4 with a magnification of 5000 times. The average particle size (d_{50}) of POP was 60 μm and the average specific surface area was 300 m^2/kg as summarized in Table 1 and are similar to the Portland Cement **[21]**.

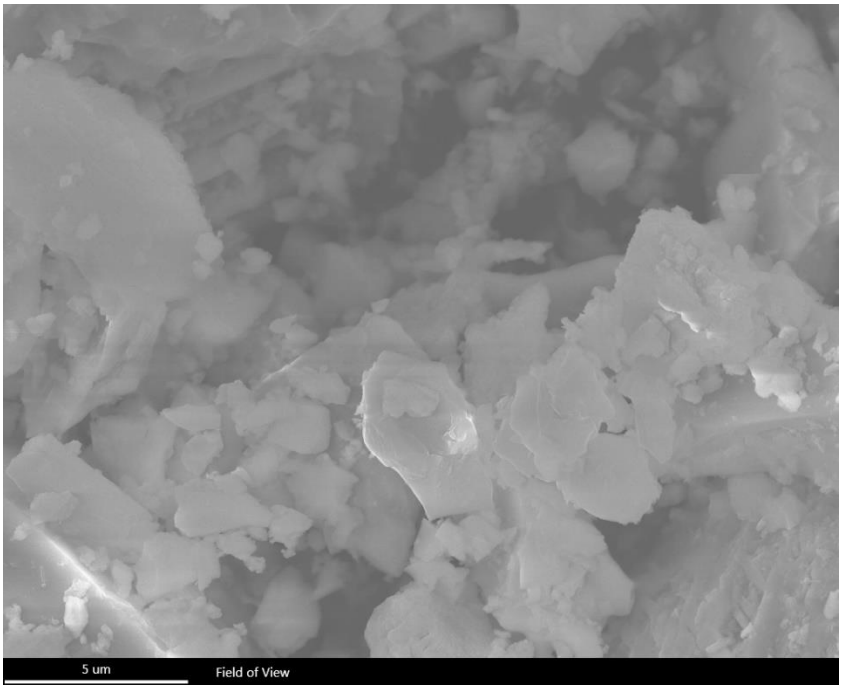

Figure 4 SEM image of Plaster of Paris Powder (magnification of 5000X).

Table 1. Physical Properties of POP Powder (from Manufacturers Data Sheets).

Property	POP

Loss of Ignition (%)	1.60
Average particle size, µm	60.0
Specific gravity	2.54
Specific Surface, m^2/kg	300
Water Solubility (%)	0.3

Chemistry

It was also important to characterize the chemical composition of the P-O-P powder to understand **the** similarities and differences compared to **the Portland cement**. The EDS was used to determine the chemical compositions of the P-O-P powder. The test results are summarized in Table 2.

Based in the weight percentage, Oxygen (O) was the highest followed by Calcium (Ca) and Sulfur (S). Based on the atomic content, oxygen (O) was the highest similar to the **Portland cement**. The sulfur (S) content by weight (22.1%) much higher than Portland Cement (about 3%).

Table 2. Chemical Composition of POP Based on the Energy Dispersive Spectroscopic (EDS) Analyses.

Element	Weight (%)	Atomic (%)
Ca (%)	27.59	13.33
S (%)	22.07	13.33
O (%)	49.66	60.00
H (%)	0.68	13.33

Electrical Characterization the P-O-P:

The **impedance-frequency** responses for the P-O-P material slurry (zero time) and 28 days after curing **are shown in Figure 5 and Figure 6 respectively**.

Zero Time: Immediately after mixing, the impedance was measured at different frequencies and the changes are shown in Figure 5. It clearly indicated that P-O-P slurry **was** CASE 2. The Vipulanandan impedance model (Eqn. 3) with at least 15 data was used with the least square method to determine the contact resistances and capacitance and the P-O-P resistance and assuming the contacts were not the same. During the statistical process the root mean square error (RMSE) was used to minimize the error and the contact resistances were about 400 Ω as summarized in the **Figure 5 data box** and Table 3. The bulk resistance of P-O-P slurry was 56.2 Ω, and the contact resistances were about 7 times higher than the bulk resistance.

28 days: The impedance was measured at different frequencies and the changes are shown in Figure 6. It clearly indicated that P-O-P solid **was** CASE 2. The Vipulanandan impedance model (Eqn. 3) with at least 15 data was used with the least square method to determine the contact resistances and capacitance and the P-O-P resistance and assuming the contacts were not the same. During the statistical process the RMSE was used to minimize the error and the contact resistances were in the range of 1700 Ω to 1720 Ω as summarized in the Figure 6 data box ~~and Table 3~~. The bulk resistance of the solidified P-O-P slurry was 522.3 Ω, and the contact resistances were over 3 times higher than the bulk resistance. In 28 days of curing the bulk resistance increased by 829%, clearly indicating the sensitivity of resistance and resistivity of the P-O-P material.

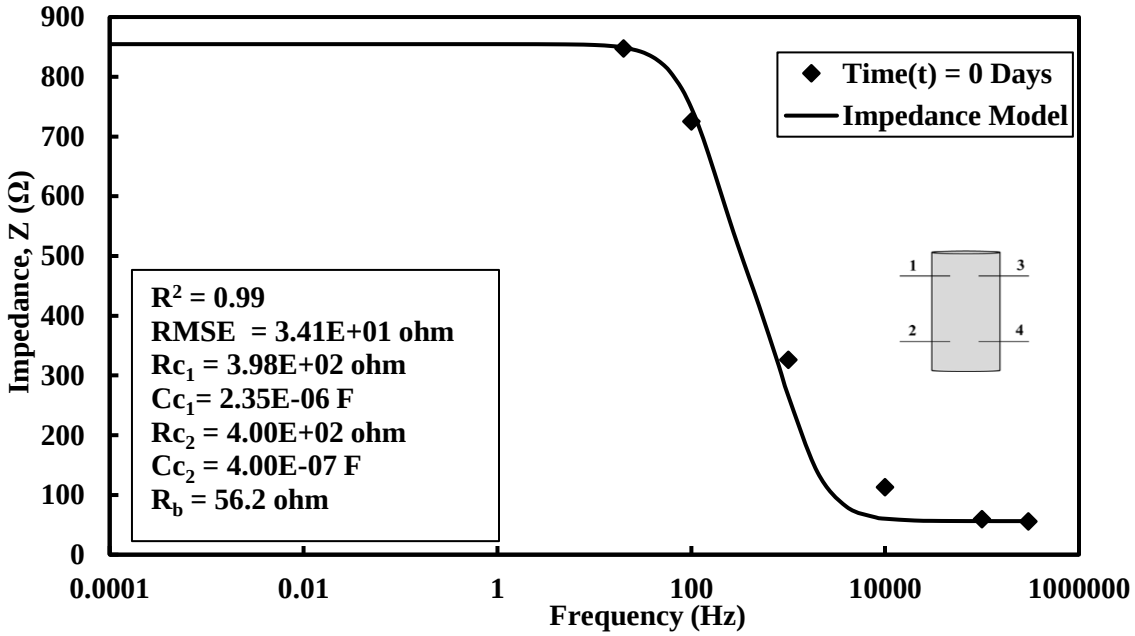

Figure 5. Electrical Impedance (Vertical 1-2) for the P-O-P material at time (t) = 0 Days.

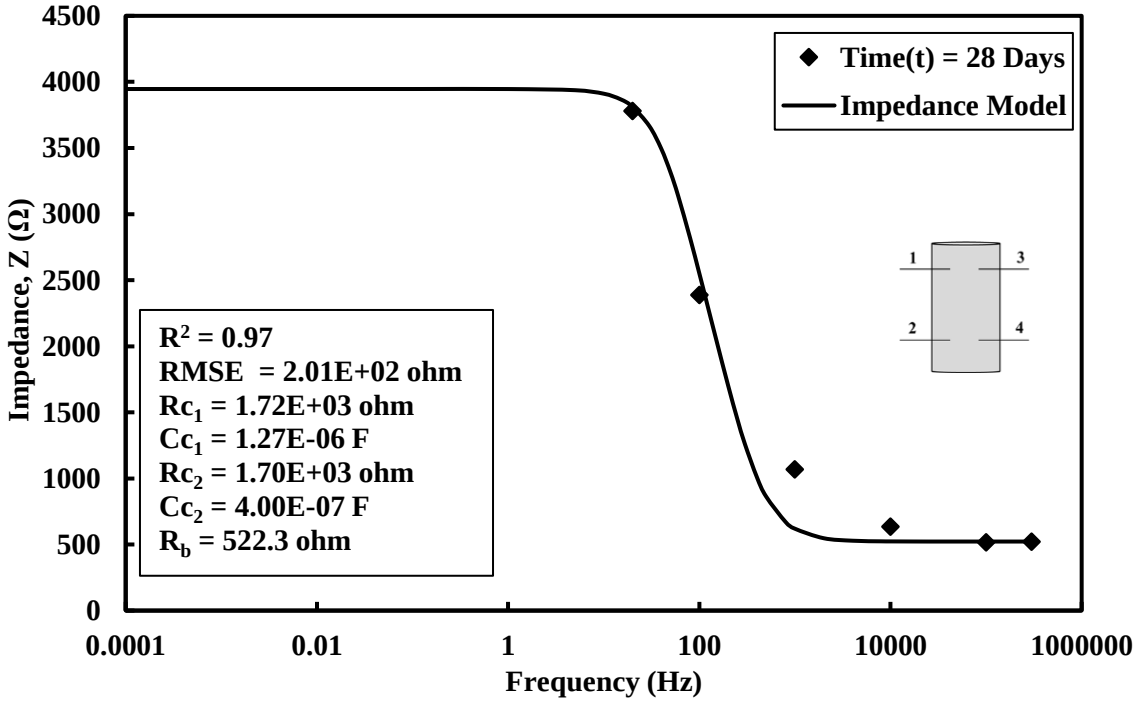

Figure 6. Electrical Impedance (Vertical 1-2) for the Solified P-O-P after 28 Days.

Curing of P-O-P

The P-O-P with and without CF was monitored for 28 days of curing. Immediately after mixing the P-O-P with and without carbon fibers Initial resistivity was measured. During the curing the resistivity rapidly changed with the time as shown in Figure 7. There are several parameters that can be used in monitoring the curing (hardening process) of the P-O-P material. Some of the parameters are initial resistivity (ρ_o), minimum resistivity (ρ_{min}), time to reach the minimum resistivity (t_{min}) and resistivity after 24 hours of curing (ρ_{24}). After initial mixing, the electrical resistivity reduced to a minimum value (ρ_{min}), and then it gradually increased with time. Time to reach minimum resistivity, t_{min}, can be used as an index of speed of chemical reactions and P-O-P material setting times. The RI_{24} is the resistivity index, indicates the maximum percentage change in resistivity in the first 24 hours of curing [**21**]. With the formation of resistive solid hydration products which block the conduction path, resistivity increased sharply with curing time [9]. The following increase in electrical resistivity was caused by the formation of large amounts of gypsum products in the P-O-P matrix. Finally, a relatively stable increase in trend was reached by the ions diffusion control of hydration process, and resistivity increased steadily with the curing time. The electrical resistivity was modeled using the Vipulanandan Curing Model (Eqn. (5)).

P-O-P Only: The initial resistivity (ρ_o) for the P-O-P with water-to-binder ratio of 0.5 and without carbon fibers was 3.29 Ω-m immediately after the mixing. It was also the minimum resistivity (ρ_{min}) and hence the time to reach the minimum resistivity (t_{min}) was also zero as summarized in Table 4. Also these are indicators of the quality of mixing. In 24 hours of curing the resistivity was 22.3 ohm.m, 577% change, representing the RI_{24}. The resistivity after 28 days of curing was 28.12 ohm.m for the P-O-P, more than 754% increase compared to the initial resistivity.

0.02% Carbon Fibers: The initial resistivity (ρ_o) for the P-O-P with water-to-binder ratio of 0.5 and with 0.02% carbon fibers (based on weight of P-O-P) was 1.47 Ω-m immediately after the mixing. It was also the minimum resistivity (ρ_{min}) and hence the time to reach the minimum resistivity (t_{min}) was also zero as summarized in Table 4. Also these are indicators of the quality of mixing. In 24 hours of curing the resistivity was 11.2 Ω-m, 662% change, representing the RI_{24}. The resistivity after 28 days of curing was 14.89 Ω.m for the P-O-P with 0.02% carbon fibers, more than 913% increase compared to the initial resistivity.

0.05% Carbon Fibers: The initial resistivity (ρ_o) for the P-O-P with water-to-binder ratio of 0.5 and with 0.05% carbon fibers (based on weight of P-O-P) was 0.89 Ω-m immediately after the mixing. It was also the minimum resistivity (ρ_{min}) and hence the time to reach the minimum resistivity (t_{min}) was also zero as summarized in Table 4. Also these are indicators of the quality of mixing. In 24 hours of curing the resistivity was 6.23 Ω-m, 600% change, representing the RI_{24}. The resistivity after 28 days of curing was 8.27 Ω.m for the P-O-P with 0.05% carbon fibers, more than 829% increase compared to the initial resistivity.

Vipulanandan Curing Model: Model parameters p_1 and q_1 decreased with the addition of conductive fillers for the P-O-P material. The model parameter p_1 varied from 0.456 to 0.878, while parameter q_1 varied from 0.085 to 0.121 (Table 4). This model predicted the curing trend very well (Figure 7). The coefficient of determination (R^2) varied was 0.99 and the RMSE (root mean square error) varied in the range of was 1.17 to 1.9 Ω.m.

Table 4. Curing model parameters for smart orthopedic cast material for 28 days of curing.

Orthopedic Cast Material	Initial Resistivity, ρ_o (Ω-m)	ρ_{min} (Ω-m)	t_{min} (min)	t_o (min)	$\rho_{24\,h}$ (Ω-m)	RI_{24} (%)	p_1	q_1

CF = 0%	3.29	3.29	0	0.001	22.3	577	0.878	0.121
CF = 0.02%	1.47	1.47	0	0.001	11.2	662	0.456	0.085
CF = 0.05%	0.89	0.89	0	0.001	6.23	600	0.624	0.101

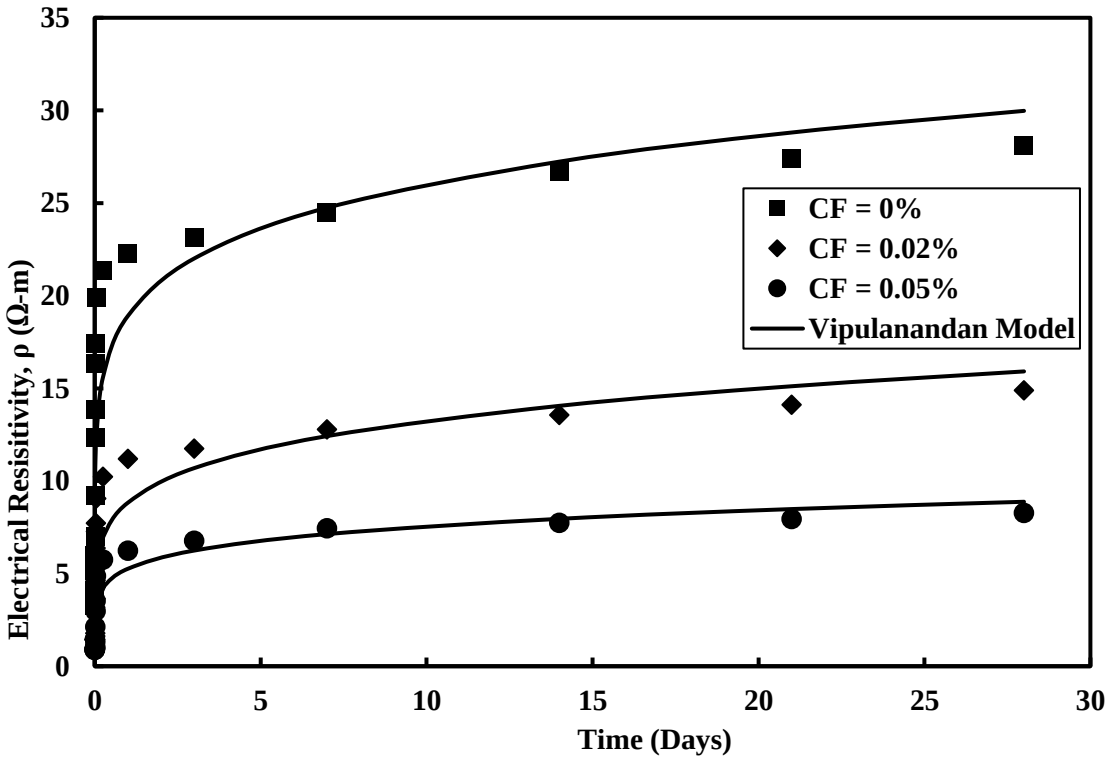

Figure 7. Variation of the Electrical Resistivity Changes of the Smart P-O-P Materials during the 28 days of curing.

Compressive Stress- Piezoresistive Strain

In order to monitor, it is important to test and quantify the piezoresistive behavior of the smart P-O-P material. The specimens were cured under room condition and the stress- piezoresistive strain responses were non-linear.

1 Day of Curing

P-O-P Only: The piezoresistive axial strain for the P-O-P without any carbon fibers was 0.76% at a peak compressive stress of 2.14 MPa after 1 day of curing as summarized in Table 5 and also compared in Figure 8. The secant piezoresistive modulus at peak stress (ratio of failure stress (σ_f) /failure piezoresistive axial strain $(\Delta\rho/\Delta\rho_0)_0$) was 282 MPa. The initial piezoresistive modulus was 329 MPa. The ratio of secant modulus to initial modulus was 0.855 indicating the non-linearity of the stress-piezoresistive strain relationship [9].

0.02% Carbon Fibers: The piezoresistive axial strain for the P-O-P with 0.02% carbon fibers was 341% at a peak compressive stress of 2.25 MPa after 1 day of curing as summarized in Table 5 and compared in Figure 8. So addition of 0.02% carbon fibers increased the compressive strength by over 5%. Addition of 0.02% carbon fibers increased the piezoresisitive strain by over 447 times (44,700%),

clearly indicating the piezoresistive behavior and also the sensitivity of resistivity. The secant piezoresistive modulus at peak stress (ratio of failure stress (σ_f) /failure piezoresistive axial strain $(\Delta\rho/\Delta\rho_0)_0$) was 0.66 MPa. The initial piezoresistive modulus was 0.75 MPa. The ratio of secant modulus to initial modulus was 0.885 indicating the non-linearity of the stress-piezoresistive strain relationship but it was more linear than the P-O-P only material behavior.

0.05% Carbon Fibers: The piezoresistive axial strain for the P-O-P with 0.05% carbon fibers was 383.2% at a peak compressive stress of 2.33 MPa after 1 day of curing as summarized in Table 5 and compared in Figure 8. So addition of 0.05% carbon fibers increased the compressive strength by over 8.9%. Addition of 0.05% carbon fibers increased the piezoresisitive strain by over 503 times (50,300%), clearly indicating the piezoresistive behavior and also the sensitivity of resistivity. The piezoresistivity strain change per unit stress was 164%/MPa after 7 days of curing.The secant piezoresistive modulus at peak stress (ratio of failure stress (σ_f) /failure piezoresistive axial strain $(\Delta\rho/\Delta\rho_0)_0$) was 0.60 MPa. The initial piezoresistive modulus was 0.65 MPa. The ratio of secant modulus to initial modulus was 0.93 indicating the non-linearity of the stress-piezoresistive strain relationship but it was more linear than the P-O-P only material behavior.

Vipulanandan Piezoresistive p-q Model: The piezoresistivity of smart P-O-P was modeled using the Vipulanandan piezoresistivity model (Eqn. 6). The model parameter p_2 decreased from 0.12 to 0.06 while the model parameter q_2 increased from 0.855 to 0.93 after 1 day of curing with varying carbon fiber contents (Table 5). Vipulanandan piezoresistivity predicted the piezoresistivity trend very well as shown in Figure 8. The coefficient of determination (R^2) was 0.99 and the RMSE (root mean square error) varied in the range of **0.050** to 0.056 MPa as summarized in Table 5.

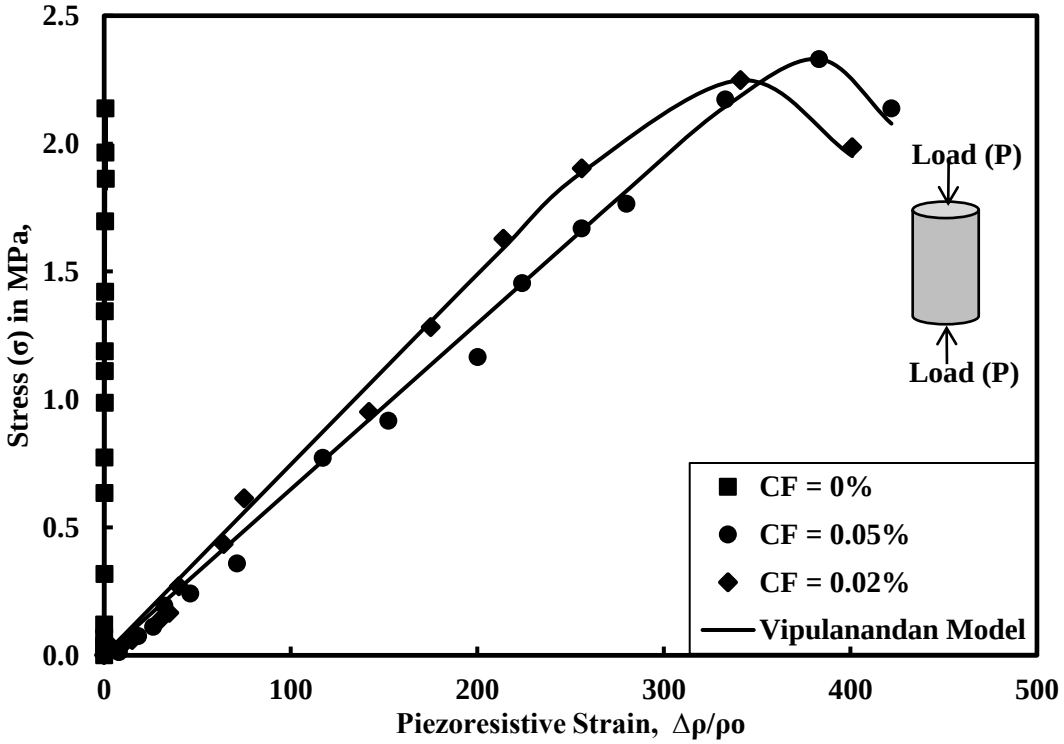

Figure 8. Behavior of smart Piezoresistive P-O-P Materials with Vary Carbon Fiber Contents After 1 day of Curing.

Table 5. Piezoresistivity model parameters for smart P-O-P material for 1 day of curing.

1 Day Piezoresistivity Model						
P-O-P Material	p_2	q_2	σc_{max} (MPa)	$\Delta\rho/\rho_o$ (%)	R^2	RMSE (MPa)
CF = 0%	0.12	0.855	2.14	0.76	0.99	0.055
CF = 0.02%	0.115	0.885	2.25	341	0.99	0.050
CF = 0.05%	0.06	0.93	2.33	383.2	0.99	0.056

28 Days of Curing

P-O-P Only: The piezoresistive axial strain for the P-O-P without any carbon fibers was 0.68% at the peak compressive stress of 6.04 MPa after 28 days of curing as summarized in Table 7 and compared in Figure 10. The secant piezoresistive modulus at peak stress (ratio of failure stress (σ_f) /failure piezoresistive axial strain $(\Delta\rho/\Delta\rho_0)_0$) was 888 MPa, over three times higher than the 1 day cured P-O-P with without carbon fibers. The initial tangent piezoresistive modulus was 945 MPa, about 3 times higher than the 1 day cured P-O-P without carbon fibers. The ratio of secant modulus to initial modulus was 0.94 indicating the non-linearity of the stress-piezoresistive strain relationship and it was more linear than the 1 day cured P-O-P [9].

0.02% Carbon Fibers: The piezoresistive axial strain for the P-O-P with 0.02% carbon fibers was 311% at a peak compressive stress of 6.15 MPa after 28 days of curing as summarized in Table 7 and compared in Figure 10. Addition of 0.02% carbon fibers increased the compressive strength by about 2%, compared to the P-O-P without fibers. Addition of 0.02% carbon fibers increased the piezoresisitive strain at failure to 311%, over 457 times (45,700%) compared to the P-O-P without fibers, clearly indicating the piezoresistive behavior of smart P-O-P and also the sensitivity of resistivity. The piezoresistivity strain change per unit stress was 50.5 %/MPa after 28 days of curing. The secant piezoresistive modulus at peak stress (ratio of failure stress (σ_f) /failure piezoresistive axial strain $(\Delta\rho/\Delta\rho_0)_0$) was 1.98 MPa. The initial tangent piezoresistive modulus was 2.18 MPa. The ratio of secant modulus to initial modulus was 0.908 indicating the non-linearity of the stress-piezoresistive strain relationship.

0.05% Carbon Fibers: The piezoresistive axial strain for the P-O-P with 0.05% carbon fibers was 345% at a peak compressive stress of 6.28 MPa after 28 days of curing as summarized in Table 7 and compared in Figure 10. So addition of 0.05% carbon fibers increased the compressive strength by over 4% compared to the P-O-P without fibers. Addition of 0.05% carbon fibers increased the piezoresisitive strain by over 507 times (50,700%) compared to the P-O-P without carbon fibers, clearly indicating the piezoresistive behavior of the smart P-O-P and also the sensitivity of resistivity. The piezoresistivity strain change per unit stress was 54.9 %/MPa after 28 days of curing. The secant piezoresistive modulus at peak stress (ratio of failure stress (σ_f) /failure piezoresistive axial strain $(\Delta\rho/\Delta\rho_0)_0$) was 1.82 MPa. The initial piezoresistive modulus was 1.92 MPa. The ratio of secant modulus to initial modulus was 0.946 indicating the non-linearity of the stress-piezoresistive strain relationship.

Vipulanandan Piezoresistive p-q Model: The piezoresistivity of smart P-O-P was modeled using the Vipulanandan piezoresistivity model (Eqn. 6). The model parameter p_2 decreased from 0.091 to 0.053 while the model parameter q_2 varied from 0.908 to 0.946 after 28 days of curing with the increase in carbon fiber contents (Table 7). Vipulanandan piezoresistive p-q model predicted the piezoresistivity trend very well as shown in Figure 10. The coefficient of determination (R^2) varied from 0.98 to 0.99 and the RMSE (root mean square error) varied in the range of 0.179 to 0.278 MPa as summarized in Table 7.

The piezoresistive strain for the P-O-P material was 0.68 % at a peak compressive stress of 6.04 MPa after 28 days of curing. This demonstrated that the P-O-P material was not sensitive to applied stress. With addition of 0.02% conductive filler, the piezoresistive strain for orthopedic cast material was 311% at a peak compressive stress of 6.15 MPa after 28 days of curing. Hence, the piezoresistivity per unit stress was 50.5 %/MPa in the lab samples after 28 days of curing. Addition of 0.05% conductive filler further increased the piezoresistive strain of P-O-P material to 345% at a peak compressive stress of 6.28 MPa, showing piezoresistivity per unit stress was 54.9 %/MPa after 28 days of curing (Figure 10). The piezoresistivity of smart P-O-P material was modeled using **the** Vipulanandan piezoresistivity model for 28 days curing (Eqn. 6).

Table 7. Model parameters for the Piezoresistivity model for the smart P-O-P material after 28 days of curing.

28 Day Piezoresistivity Model						
P-O-P Material	p_2	q_2	σ_{cmax} (MPa)	$\Delta\rho/\rho_o$ (%)	R^2	RMSE (MPa)
CF = 0%	0.06	0.94	6.04	0.68	0.99	0.179
CF = 0.02%	0.091	0.908	6.15	311	0.98	0.278
CF = 0.05%	0.053	0.946	6.28	345	0.99	0.206

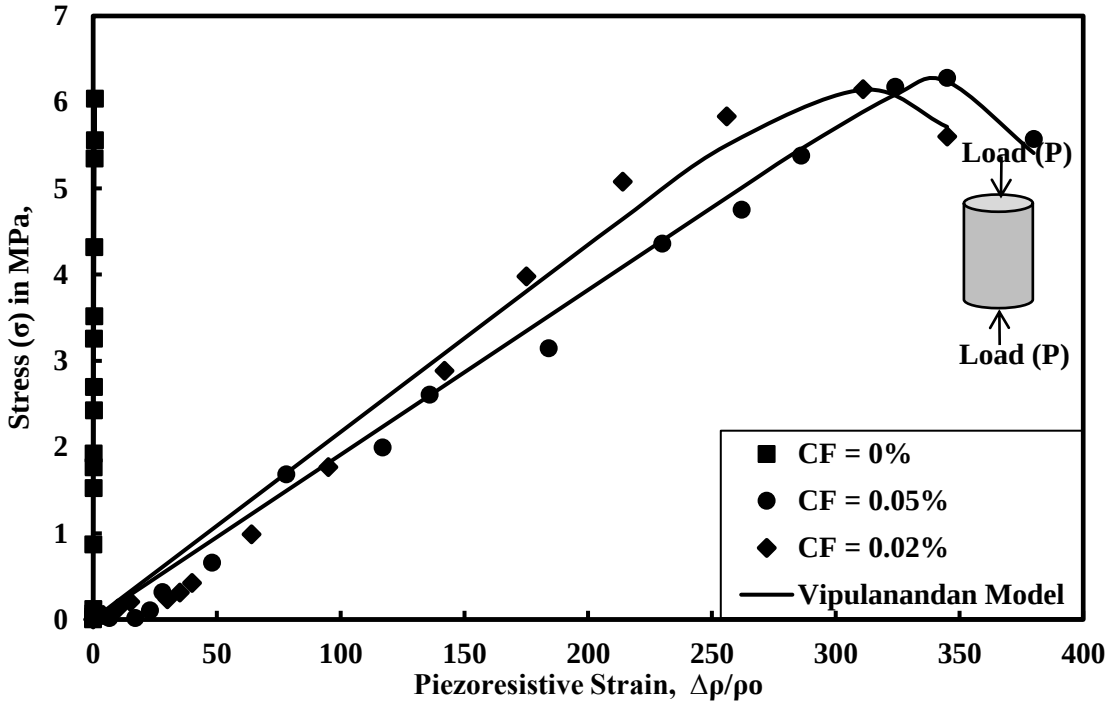

Figure 10. Behavior of Smart Piezoresistive P-O-P material after 28 days of curing.

Property Changes with Curing Time

In order to quantify the property (strength, piezoresistive strain at failure) changes with the curing time for the P-O-P with and without carbon fibers. Reviewing the data, Vipulanandan Correlation Model was selected to predict the trends. Vipulanandan Correlation Model **[19, 20, 21]** is represented as follows:

$$Y = Y_0 + \frac{t}{A+B*t} \quad (7)$$

Where t is the time and Y is the material property. Parameters Y_0, A and B are the material properties, depends on the compositions and curing environments. The long-term property (Y_∞) can be predicted when the time goes to infinity and can be represented as follows:

$$t \rightarrow \infty \qquad Y_\infty = Y_0 + \frac{1}{B} \quad (8)$$

Compressive Strength

The model parameters Y_o, A and B in Eqn. (7) will be replaced with Y_1, A_1 and B_1 respectively. Also the parameter Y_1 representing the compressive strength at zero curing was zero for all the cases. The variation of compressive strengths with curing time is shown in Figure 11.

P-O-P only: The compressive strength after one day of curing was 2.14 MPa and it increased to 4.32 MPa in 7 days, almost doubling (100%) in strength. The 28 day compressive strength was

6.04 MPa and was over 180% higher than the 1 day strength. The model Parameter A_1 was 0.377 day/MPa and the model parameter B_1 was 0.159 MPa^{-1} as summarized in Table 8. Hence the long-term strength predicted by the Model using the Eqn. (8) was 6.29 MPa.

0.02% Carbon Fibers: The compressive strength after one day of curing was 2.25 MPa and it increased to 4.49 MPa in 7 days, almost doubling (100%) in strength. The 28 day compressive strength was 6.15 MPa and was over 173% higher than the 1 day strength. The model Parameter A_1 was 0.343 day/MPa and the model parameter B_1 was 0.157 MPa^{-1} as summarized in Table 8. Hence the model parameter A_1 decreased and also parameter B_1 reduced as shown in Figure 12. Also the long-term strength predicted by the Model using the Eqn. (8) was 6.37 MPa, which was 1.3% higher than the P-O-P only.

0.05% Carbon Fibers: The compressive strength after one day of curing was 2.33 MPa and it increased to 4.61 MPa in 7 days, almost doubling (100%) in strength. The 28 day compressive strength was 6.28 MPa and was about 170% higher than the 1 day strength. The model Parameter A_1 was 0.349 day/MPa and the model parameter B_1 was 0.152 MPa^{-1} as summarized in Table 8. Hence the model parameter A_1 decreased and also parameter B_1 reduced as shown in Figure 12. Also the long-term strength predicted by the Model using the Eqn. (8) was 6.58 MPa, which was 4.6% higher than the P-O-P only.

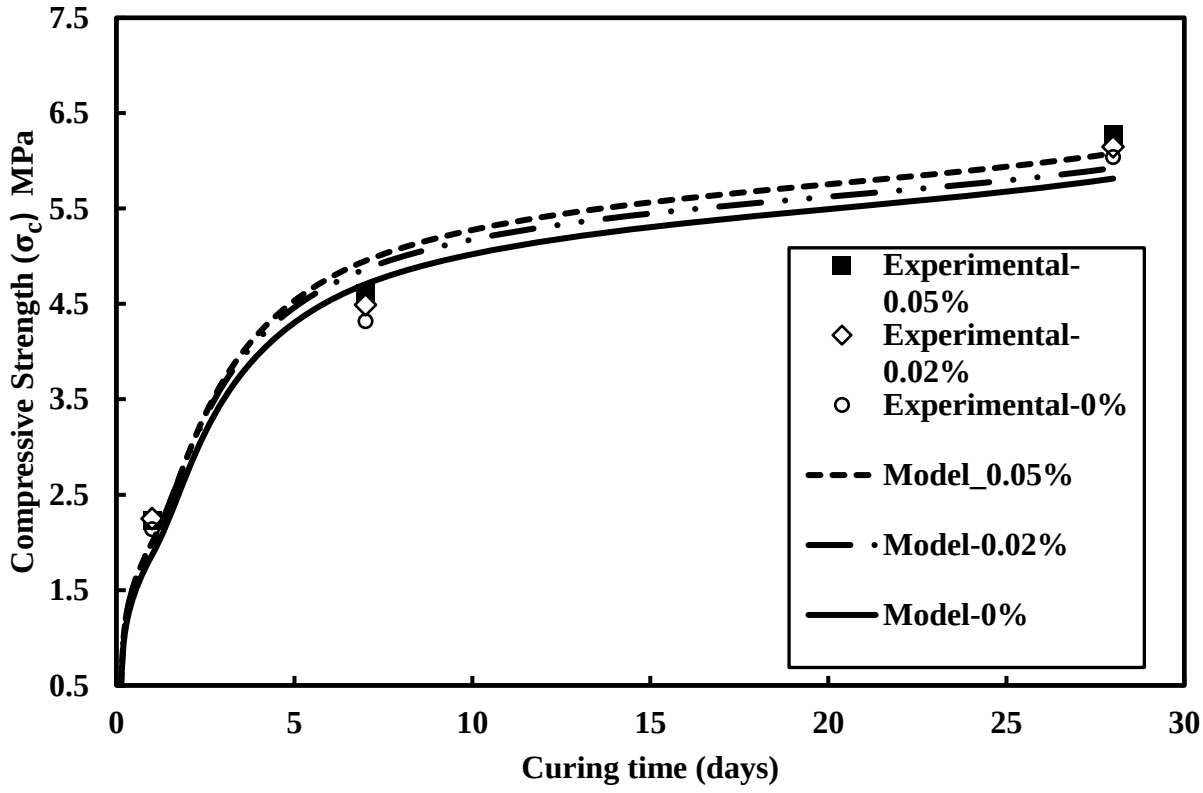

Figure 11. Measured and Predicted Variation of Compressive Strength with Curing Time

Table 8. Summary of Model Parameters for Strength Prediction of the P-O-P with and without Carbon Fibers

Material	Parameters			RMSE (MPa)	R^2
	σ_o (MPa)	A_1 (days/MPa)	B_1 $(MPa)^{-1}$		
P-O-P Only	0	0.377	0.159	0.131	0.99
0.02% CF	0	0.343	0.157	0.126	0.99
0.05% CF	0	0.349	0.152	0.115	0.99

~~**Figure 12 Variations of the Strength Model Parameters with the Carbon Fiber Contents.**~~

Piezoresistive Axial Strain at Failure

The model parameters Y_o, A and B in Eqn. (7) will be replaced with Y_2, A_2 and B_2 respectively. The variation of the piezoresistive axial strain with curing time for the smart P-O-P is shown in Figure 13.

P-O-P only: The compressive piezoresistive axial strain at failure after one day of curing was 0.76% and it decreased to 0.72% after 7 days of curing. The 28 day compressive piezoresistive axial strain at failure strength was 0.68%, over 10% decrease in the piezoresistive axial strain at failure compared to the 1 day curing. The model Parameter A_2 was 0.25 day/% and the model parameter B_2 was 0.159 $\%^{-1}$ as summarized in Table 9. The model parameter Y_2 was 0.80%. Hence the long-term compressive piezoresistive axial strain predicted by the Model using the Eqn. (8) was 0.60%.

0.02% Carbon Fibers: The compressive piezoresistive axial strain at failure after one day of curing was 341% and it decreased to 328% after 7 days of curing. The 28 day compressive piezoresistive axial strain at failure strength was 311%, 8.8% decrease in the piezoresistive axial strain at failure compared to the 1 day curing. The model Parameter A_2 was -0.123 day/% and the model parameter B_2 was -0.022 $\%^{-1}$ as summarized in Table 9. The model parameter Y_2 was 350%. The predicted trend is compared with the experimental results in Figure 12 and the RMSE and R^2 are summarized in Table 9. Hence the long-term compressive piezoresistive axial strain predicted by the Model using the Eqn. (8) was 305%., which was very much higher than the P-O-P without carbon fibers.

0.05% Carbon Fibers: The compressive piezoresistive axial strain at failure after one day of curing was 383% and it decreased to 370% after 7 days of curing. The 28 day compressive piezoresistive axial strain at failure strength was 345%, about 10% decrease in the piezoresistive axial strain at failure compared to the 1 day curing. The model Parameter A_2 was -0.174 day/% and the model parameter B_2 was -0.017 $\%^{-1}$ as summarized in Table 9. The model parameter Y_2 was 390%. The predicted trend is compared with the experimental results in Figure 13 and the RMSE and R^2 are summarized in Table 9. Hence the long-term compressive piezoresistive axial strain predicted by the Model using the Eqn. (8) was 331%,which was higher compared to the P-O-P with 0.02% carbon fibers and also very much higher than the P-O-P without carbon fibers.

Table 9. Summary of Model Parameters for the Piezoresisitive Axial Strain at failure Prediction of the P-O-P with and without Carbon Fibers

Material	Parameters			RMSE (%)	R^2
	Y_2 (%)	A_1 (days/%)	B_1 $(\%)^{-1}$		
P-O-P Only	0.80	-0.123	0.159	0.0	0.99
0.02% Carbon Fibers	350	-0.123	-0.022	0.032	0.98
0.05% Carbon Fibers	390	-0.174	-0.017	0.045	0.94

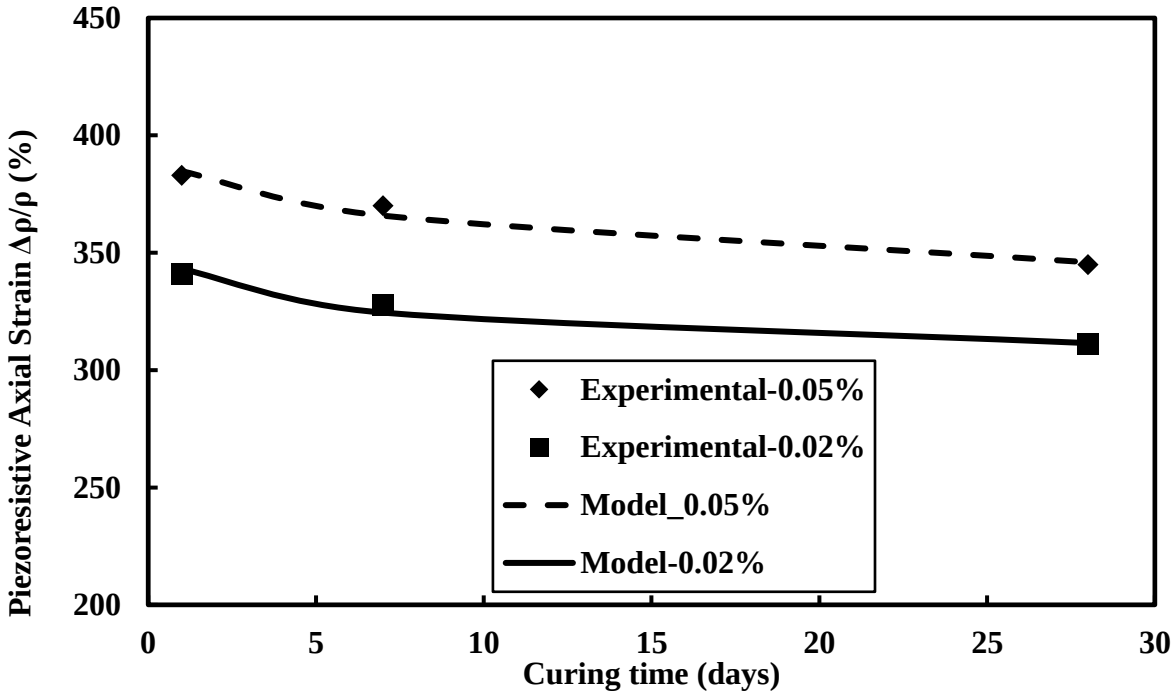

Figure 13 Measured and Predicted Variations of the Piezoresistive Axial Strain for the Smart P-O-P P with the Curing time.

4. Conclusions

Based on this study which included the experimental test results and analytical modeling of the smart piezoresistive Plaster of Paris following conclusions are advanced:

(1). Using the new material characterization method the electrical resistivity was identified as the critical material parameter for real-time monitoring the changes in the P-O-P. **Tests were performed to verify the sensitivity of resistivity during curing and solidified P-O-P.**

(2). Initial resistivity was highly sensitive to the carbon fiber addition. With the addition of 0.05% carbon fiber the initial resistivity reduced from 3.29 Ωm to 0.89 Ωm, 73% reduction.

(3). The resistivity was highly sensitive to the curing of P-O-P with and without carbon fibers. The resistivity changed by over 570% for the P-O-P only. Vipulanandan Curing Model predicted the experimental results very well.

(4). Adding 0.02% and 0.05% of carbon fibers made the P-O-P to **be a** highly piezoresistive material, smart P-O-P. With the addition of 0.05% carbon fibers the piezoresistivity strain was increased by over 500 times (50,000%) **after 28 days of curing.** The compressive stress – piezoresistive strain relationships were modelled using the Vipulanandan Piezoresistive p-q Model.

(5). Variation of piezoresistive axial failure strain and compressive strength with curing time were modelled using the Vipulanandan Correlation Model. **The compressive strengths increased with the curing time but the piezoresistive axial strain at peak stress reduced**. The ultimate piezoresistive strain **for** the P-O-P with 0.05% carbon fibers was over 300%.

Acknowledgement

This study was supported by the Center for Innovative Grouting Materials and Technology (CIGMAT) and Texas Hurricane Center for Innovative Technology (THC-IT) with funding from various industries. The study was done at the University of Houston, Houston, Texas.

References

[1] ASTM C39/C39M (2001) "Compressive Strength of Cylindrical Concrete Specimens," ASTM Committee C09, West Conshohocken, PA 19428-2959, United States.

[2] ASTM C191 (2019) "Testing Method for Time of Setting of Hydraulic Cement by Vicat Needle," ASTM Committee C01, West Conshohocken, PA 19428-2959, United States.

[3] Browner, B. D., Jupiter, J. B., Levine, A. M., Trafton, P. G., Krettek, C. and Green, N. E. (2008). "The history of fracture treatment." Skeletal Trauma. pp. 1–32.

[4] Camarini, G. and J. A. D. Milito, (2011) "Gypsum hemihydrate–cement blends to improve renderings durability," Construction and Building Materials, Vol. 25, No. 11, pp. 4121–4125.

[5] Hernandez-Olivares, F. Bollati, M. R., Rio, M. and Paraga-Landa, B. (1999), "Development of Cork-Gypsum Composites for Building Applications, Construction and Building Materials, Vol. 13, pp. 179-186.

[6] Lanzon, M. and Garcia-Ruiz, P.A. (2012), "Effect of Citric Acid on Setting Inhibition and Mechanical Properties of Gypsum Building Plasters," Construction and Building Materials, Vol. 28, pp. 506-511.

[7] Lewry, A. J. and Williamson, J. (1994). "The setting of gypsum plaster: Part II – The development of microstructure and strength," Journal of Material Science, Vol. 29, pp. 5524-5528.

[8] Li, Z., Xu, K., Peng, J., J Wang, J., Ma, X. and Niu, J. (2018). Study on Hydration and Mechanical Property of Portland Cement-Blended Recycled Plaster Materials" Advances in Materials Science and Engineering, Hindawi, Article ID 2692347 | https://doi.org/10.1155/2018/2692347.

[9] Maddi A.R., Vipulanandan, C. and Mohan, C. (2022). Compressive Behavior of Plaster of Paris Used for Orthopedic Casting and Multiple Infrastructure Applications.' CIGMAT Conference Proceedings, pp. II-34 -40, (http://cigmat.uh.edu)

[10] Parmar, A. J., Tyagi, S. K., Dabas, V. S., Mistry, J. N., Jhala, S. K., Suthar, D. N., Bhatt, R. H., Pansuria, R. H. and Bhatti, I. M. (2014). "Assessment of the physical and mechanical properties of plaster of Paris bandage cast used as a splinting and casting materials." Veterinary World, pp. 1123-1126.

[11] Parres, F., Crespo-Amoros, J.E. and Nadal-Gisbert, A. (2009) Mechanical Properties Analysis of Plaster Reinforced with Fibers and Microfibers Obtained From Shredded Tires," Construction and Building Materials, Vol. 23, pp. 3182-3188.

[12] Piro, N.S., Mohammed, A.S. and Hamad S.M.(2023), Compressive Strength and Piezoresistivity of Smart Cement Paste Modified with Waste Steel Slag, Journal of Building Engineering, Volume 70, https://doi.org/10.1016/j.jobe.2023.106393.

[13] Piro N.S., Mohammed, A., Samir M. Hamad, S.M. and Rawaz Kurda, R. (2022) Electrical Resistivity-Compressive Strength Predictions for Normal Strength Concrete with Waste Steel Slag as a Coarse Aggregate Replacement using Various Analytical Models," Construction and Building Materials, Volume 327, https://doi.org/10.1016/j.conbuildmat.2022.127008.

[14] Sophia, M., Sakehieswaran, N. and Ganesh Babu, O. (2016), "Gypsum as a Construction Material –A Review of Recent Developments," International Journal for Innovative Research in Science $ Technology, Vol. 2 No. 12, pp. 315 – 323.

[15] Szostakowski, B., Smitham, P. and Khan, W. S. (2017). "Plaster of Paris – Short History of Casting and injured limb immobilization." The Open Orthopaedics Journal, vol. 11, pp. 291-296.

[16] Vipulanandan, C. and Prashanth, P. (2013). "Impedance Spectroscopy Characterization of a Piezoresistive structural Polymer Composite Bulk Sensor." Journal of Testing and Evaluation, ASTM, Vol. 41, pp. 898-904.

[17] Vipulanandan, C., and Ali, K., (2018) "Smart Cement Grouts for Repairing Damaged Piezoresistive Cement and the Performances Predicted Using Vipulanandan Models" Journal of Civil Engineering Materials**,** American Society of Civil Engineers (ASCE), Vol. 30, No. 10, Article number 04018253.

[18] Vipulanandan, C., and Amani, N. (2018) "Characterizing the Pulse Velocity and Electrical resistivity Changes In Concrete with Piezoresistive Smart Cement Binder Using Vipulanandan Models" Construction and Building Materials, Vol. 175, pp. 519-530.

[19] Vipulanandan, C. and Mohammed, A. (2020), "Magnetic Field Strength and Temperature Effects on the Behavior of Oil Well Cement Slurry Modified with Iron Oxide Nanoparticles and Quantified with Vipulanandan Models", Journal of Testing and Evaluation. Vol. 48(6), pp. 4516-4537.

[20] Vipulanandan, C., and Mohammed, A. (2015) "Smart Cement Modified With Iron Oxide Nanoparticles to Enhance the Piezoresistive Behavior and Compressive Strength for Oil Well Applications." Journal of Smart Materials and Structures, Vol. 24 Number 12, pp. 1-11.

[21] Vipulanandan, C. (2021) Smart Cement" Development, Testing, Modeling and Real Time Monitoring, Taylor and Francis Group, CRC Press, London, England 440 pp.

[22] Vipulanandan, C, Maddi, A.R. and Chandra Mohan (2024) Smart Piezoresistive Plaster of Paris for Real-time Monitoring of Curing and Compressive Stress Changes Quantified Using Vipulanandan Models, Journal of Material Performance and Engineering, Vol 33 (17) pp. 9059-9069, https://doi.org/10.1007/s11665-023-08640-8

[23] Yu, Q.L., Brouwers, H. J. (2011), "Microstructural and Mechanical Properties of β-hemihydrate Produced Gypsum: An insight from its Hydration Process," Construction and Building Materials, Vol. 25, pp. 3149-3157.

[24] Yu, Q.L. and Brouwers, H.J. (2012), 'Thermal properties and microstructure of gypsum board and its dehydration products: A theoretical and experimental investigation', Fire and Materials 36(7), 575–589. https://doi.org/10.1002/fam.1117.